Conformal Boundary Conditions of Symmetry-Enriched Quantum Critical Spin Chains

Xue-Jia Yu [1,*], Rui-Zhen Huang [2,3,*], Hong-Hao Song [2], Limei Xu, [1,4,5] Chengxiang Ding, [6] and Long Zhang [2,†]

[1]*International Center for Quantum Materials, School of Physics, Peking University, Beijing 100871, China*
[2]*Kavli Institute for Theoretical Sciences and CAS Center for Excellence in Topological Quantum Computation,*
University of Chinese Academy of Sciences, Beijing 100190, China
[3]*Department of Physics and Astronomy, Ghent University, Krijgslaan 281, 9000 Gent, Belgium*
[4]*Collaborative Innovation Center of Quantum Matter, Beijing 100871, China*
[5]*Interdisciplinary Institute of Light-Element Quantum Materials and Research Center for Light-Element Advanced Materials,*
Peking University, Beijing 100871, China
[6]*School of Microelectronics & Data Science, Anhui University of Technology,*
Maanshan, Anhui 243002, China

Some quantum critical states cannot be smoothly deformed into each other without either crossing some multicritical points or explicitly breaking certain symmetries even if they belong to the same universality class. This brings up the notion of "symmetry-enriched" quantum criticality. While recent works in the literature focused on critical states with robust degenerate edge modes, we propose that the conformal boundary condition (B.C.) is a more generic characteristic of such quantum critical states. We show that in two families of quantum spin chains, which generalize the Ising and the three-state Potts models, the quantum critical point between a symmetry-protected topological phase and a symmetry-breaking order realizes a conformal B.C. distinct from the simple Ising and Potts chains. Furthermore, we argue that the conformal B.C. can be derived from the bulk effective field theory, which realizes a novel bulk-boundary correspondence in symmetry-enriched quantum critical states.

Introduction.—The development of topological states of matter has greatly deepened our understanding of gapped phases [1]. For example, one-dimensional (1D) symmetry-protected topological (SPT) states are fully classified by the projective representations of the symmetry group and host degenerate edge modes, which transform as the projective representations [2,3]. Different SPT phases cannot be adiabatically connected without either crossing phase transitions or explicitly breaking the symmetry.

Quantum critical states enjoy scale invariance in the low-energy limit, and fall into different universality classes characterized by the operator scaling dimensions. Surprisingly, some quantum critical states cannot be smoothly connected by tuning model parameters without either crossing some multicritical points or explicitly breaking certain symmetries even if they belong to the same universality class. This brings up the notion of gapless SPT [4,5] or "symmetry-enriched" quantum critical states [6]. Robust degenerate edge states persist in some quantum critical states [4–20], which are secured by the symmetry-flux (disorder) operators in the bulk carrying nontrivial symmetry charges [6]. This indicates a novel bulk-boundary correspondence. However, a signature of symmetry-enriched quantum critical states without edge degeneracy is still lacking.

In this Letter, we shall show that the conformal boundary condition (B.C.) and the associated surface critical behavior are more generic characteristics of symmetry-enriched quantum criticality. For a critical system with boundary, a conformal B.C. corresponds to a fixed point of the renormalization group (RG) flow of the boundary states. Different conformal B.C. can be specified for a given conformal field theory (CFT) in the bulk, resulting in rich surface critical phenomena.

The conformal B.C. determines the operator content of the system [21,22], i.e., the Hamiltonian eigenstates, which are organized into conformal families, each comprising a primary state and all its conformal descendants. The conformal B.C. also determines the universality of the surface criticality [21,23]. Given a local operator on the boundary [denoted by $\phi(r)$] and in the bulk [$\phi_b(R)$], the connected correlation functions scale as

$$C_{\parallel}(r_1 - r_2) = \langle \phi(r_1)\phi(r_2)\rangle_c \propto |r_1 - r_2|^{-2\Delta_\phi}, \quad (1)$$

$$C_{\perp}(r - R) = \langle \phi(r)\phi_b(R)\rangle_c \propto |r - R|^{-\Delta_\phi - \Delta_\phi^b}, \quad (2)$$

in which $\langle AB \rangle_c = \langle AB \rangle - \langle A \rangle \langle B \rangle$. Here, $r_1 - r_2$ is parallel to the surface, while $r - R$ is perpendicular to it. Δ_ϕ and Δ_ϕ^b are the scaling dimensions of the boundary and the bulk

operators, respectively. The surface critical behavior of classical statistical systems has been extensively studied [24,25]. The interest in the surface criticality has been revived recently motivated by the impact of topological edge states at quantum critical points (QCPs), leading to the discovery of new universality classes [26–40].

In this Letter, we study two families of quantum spin chains, which generalize the 1D Ising and the three-state Potts models [17,18,41], respectively. Each family contains quantum critical states that are described by the same CFT but cannot be smoothly connected. While the two Ising QCPs can be distinguished by the degenerate edge states [6,17,18], the generalized Potts chain lacks such a distinctive feature. By examining their surface critical behavior and the energy and entanglement spectra, we show that in each family of models, the QCP between an SPT and a symmetry-breaking order realizes a conformal B.C. distinct from the simple Ising and Potts models. Moreover, the conformal B.C. can be derived from the effective field theory of the bulk states, thus establishing a novel bulk-boundary correspondence in symmetry-enriched quantum critical states.

Warm-up: Quantum Ising chains.—We first study the following transverse-field Ising (TFI) chain and the cluster Ising (CI) chain [18],

$$H_{\text{TFI}} = -\sum_{l=1}^{L-1} \sigma_l^z \sigma_{l+1}^z + h \sum_{l=1}^{L} \sigma_l^x, \qquad (3)$$

$$H_{\text{CI}} = -\sum_{l=1}^{L-1} \sigma_l^z \sigma_{l+1}^z - h \sum_{l=1}^{L-2} \sigma_l^z \sigma_{l+1}^x \sigma_{l+2}^z. \qquad (4)$$

Both models enjoy the $\mathbb{Z}_2 \times \mathbb{Z}_2^T$ symmetry generated by $\Pi_x = \prod_{l=1}^{L} \sigma_l^x$ and $T = \mathcal{K}$ (the complex conjugation). There is a QCP at $h_c = 1$ in both models separating the ferromagnetic (FM) order at $|h| < h_c$ and the disordered phase at $h > h_c$. The QCPs are described by the 2D Ising CFT.

Both models are exactly solvable with the Jordan-Wigner transformation [18], $\sigma_l^z = \prod_{k=1}^{l-1}(i\gamma_k \tilde{\gamma}_k)\gamma_l$ and $\sigma_l^x = i\gamma_l \tilde{\gamma}_l$, in which the Majorana fermion operators satisfy $\{\gamma_k, \gamma_l\} = \{\tilde{\gamma}_k, \tilde{\gamma}_l\} = 2\delta_{kl}$, and $\{\gamma_k, \tilde{\gamma}_l\} = 0$. In the Majorana representation,

$$H = -\sum_{l=1}^{L-1} i\tilde{\gamma}_l \gamma_{l+1} - h \sum_{l=1}^{L-\alpha} i\tilde{\gamma}_l \gamma_{l+\alpha}, \qquad (5)$$

in which $\alpha = 0$ for the TFI and 2 for the CI chain. At the QCP, both models are mapped to 1D massless Majorana fermions. However, in the CI chain, there are two decoupled Majorana modes denoted by γ_1 and $\tilde{\gamma}_L$, which lead to a twofold degeneracy in each energy level [17,18]. These edge zero modes are protected by the $\mathbb{Z}_2^T$ symmetry [6]. In the spin representation, the degeneracy comes from the conservation of the edge spin operators $\sigma_1^z = \gamma_1$ and $\sigma_L^z = -i\tilde{\gamma}_L \Pi_x$, which label the edge magnetization.
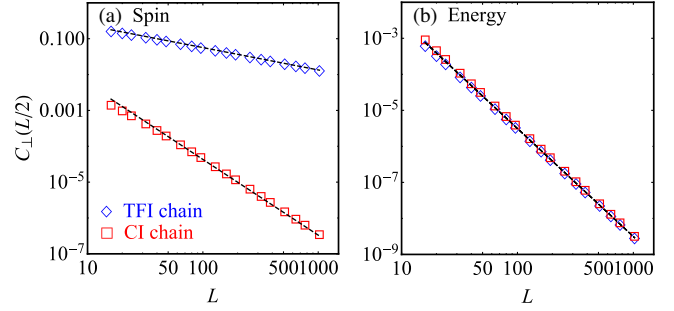

FIG. 1. Connected correlation functions $C_\perp(L/2)$ of (a) the spin operator σ_l^z and (b) the energy operator $\epsilon_l = \sigma_l^z \sigma_{l+1}^z$ of the critical Ising chains. Dashed lines are the power-law fitting according to Eq. (2).

The energy spectrum falls into four sectors labeled by σ_1^z and σ_L^z. Therefore, the $\mathbb{Z}_2$ symmetry is spontaneously broken on the edges.

The connected correlation functions $C_\perp(L/2)$ of the spin operator σ_l^z and the energy operator $\epsilon_l = \sigma_l^z \sigma_{l+1}^z$ are used to characterize the surface critical behavior. These correlations are calculated in the Majorana representation, which is detailed in Supplemental Material [42], and fitted to Eq. (2) with the bulk scaling dimensions $\Delta_\sigma^b = 1/8$ and $\Delta_\epsilon^b = 1$ (see Fig. 1). The extracted scaling dimensions of the boundary operators are listed in Table I. While the TFI chain is captured by the Ising CFT with free B.C., the exponents of the CI chain are consistent with the fixed B.C., which can be attributed to the spontaneous edge magnetization. This feature should also apply to other 1D quantum critical states with edge degeneracy.

The energy spectra with open boundaries are shown in Fig. 2. With proper normalization, the excitation energies are mapped to the operator scaling dimensions and compared with the operator content of the boundary CFT, which is explained in the figure caption. These spectra are fully consistent with the Ising CFT with free B.C. and fixed B.C., respectively.

TABLE I. Scaling dimensions of the boundary spin and energy operators. Scaling dimensions in the Ising and Potts boundary CFTs are also listed for comparison.

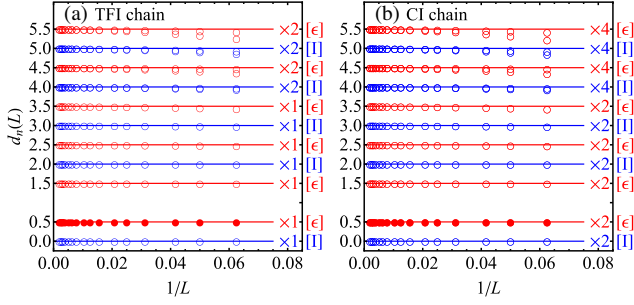| Class	Model or B.C.	Δ_σ	Δ_ϵ
Ising	TFI	0.499 2(3)	1.999 57(8)
	CI	1.998 4(2)	2.000 08(2)
CFT	Free	1/2	2
	Fixed	2	2
Potts	Disorder-FM	0.665 98(3)	0.799 3(2)
	Disorder-NotA	0.662 9(1)	0.791 5(5)
	RSPT-FM	0.066 1(3)	0.204(9)
	RSPT-NotA	0.060 1(1)	0.21(1)
CFT	Free	2/3	4/5
	Dual-mixed	1/15	1/5

FIG. 2. Low-energy spectra of (a) the TFI and (b) the CI chains with open boundaries. The excitation energy $\Delta\epsilon_n(L) = \epsilon_n(L) - \epsilon_0(L)$ is normalized to the effective scaling dimension, $d_n(L) = \frac{1}{2}[\Delta\epsilon_n(L)/\Delta\epsilon_1(L)]$, such that the first excited state (marked with filled circles) maps to $1/2$. The conformal family and the expected degeneracy in the boundary CFT are labeled on the right. The operator content in (a) is $[\mathbb{I}] \oplus [\epsilon]$, consistent with the Ising CFT with free B.C. [21]. In (b), the energy levels in blue come from $(\sigma_1^z, \sigma_L^z) = (+, +)$ and $(-, -)$ sectors, each forming a conformal family $[\mathbb{I}]$, while those in red from $(+, -)$ and $(-, +)$ sectors, each forming $[\epsilon]$. This is consistent with the fixed B.C. [21].

Generalized Potts chain: Recapitulation.—We then study the 1D generalized three-state Potts model introduced in Ref. [41]. Following their notation, the Hamiltonian is given by

$$H = H_P + \lambda H_0, \quad (6)$$

in which H_P is the simple quantum Potts model,

$$H_P = -J \sum_{l=1}^{L-1} (\sigma_l^\dagger \sigma_{l+1} + \sigma_l \sigma_{l+1}^\dagger) - f \sum_{l=1}^{L} (\tau_l + \tau_l^\dagger), \quad (7)$$

and H_0 is given by

$$H_0 = \sum_{l=1}^{L-1} 3[(S_l^+ S_{l+1}^-)^2 - S_l^+ S_{l+1}^- + \text{H.c.}] - \sum_{l=1}^{L} (\tau_l + \tau_l^\dagger). \quad (8)$$

The operators are defined by $\tau = \text{diag}(1, \omega, \omega^2)$ with $\omega = e^{2\pi i/3}$, and

$$\sigma = \begin{pmatrix} 0 & 1 & 0 \\ 0 & 0 & 1 \\ 1 & 0 & 0 \end{pmatrix}, \quad S^+ = \begin{pmatrix} 0 & 0 & 1 \\ 1 & 0 & 0 \\ 0 & 0 & 0 \end{pmatrix} = (S^-)^\dagger. \quad (9)$$

$S^\pm$ are the ladder operators of $S^z = \text{diag}(0, 1, -1)$. The model (6) enjoys the S_3 symmetry generated by the $\mathbb{Z}_3$ rotation $R = \prod_{l=1}^{L} \tau_l$ and the charge conjugation $C = \prod_{l=1}^{L} c_l$, in which

$$c = \begin{pmatrix} 1 & 0 & 0 \\ 0 & 0 & 1 \\ 0 & 1 & 0 \end{pmatrix}. \quad (10)$$

Let us first recapitulate the phase diagram of the model (6), and refer to Ref. [41] for the detailed derivation. The quantum phase diagram parametrized by $\lambda = 1 - \alpha$, $J = \alpha + \beta$, and $f = \alpha - \beta$ is sketched in Fig. 3(a), which shows four gapped phases. Each phase is adiabatically connected to a special point within the phase, $(\alpha, \beta) = (\pm 1, \pm 1)$, where the ground states can be exactly constructed. The Potts ferromagnetic (FM) ordered phase has threefold degenerate ground states, which are smoothly connected to the fully polarized FM states $\otimes_l |A\rangle_l$, $\otimes_l |B\rangle_l$ and $\otimes_l |C\rangle_l$, in which $|A\rangle$, $|B\rangle$, and $|C\rangle$ are the eigenstates of σ with eigenvalues 1, ω, and ω^2, respectively. The FM order is characterized by the order parameter $\langle\sigma_l\rangle^3 > 0$. The disordered phase is smoothly connected to the S_3-symmetric state $\otimes_l |0\rangle_l$, in which $|0\rangle = (1/\sqrt{3})(|A\rangle + |B\rangle + |C\rangle)$ is an eigenstate of S^z. The other two phases are quite unconventional. The "not-A" ordered phase contains $(\alpha, \beta) = (-1, -1)$, where the threefold degenerate ground states are given by $\otimes_l |\bar{A}\rangle_l$, $\otimes_l |\bar{B}\rangle_l$, and $\otimes_l |\bar{C}\rangle_l$, with $|\bar{A}\rangle = (1/\sqrt{2})(|B\rangle + |C\rangle)$, $|\bar{B}\rangle = (1/\sqrt{2})(|C\rangle + |A\rangle)$, and $|\bar{C}\rangle = (1/\sqrt{2})(|A\rangle + |B\rangle)$. The S_3 symmetry is spontaneously broken with the order parameter $\langle\sigma_l\rangle^3 < 0$. The last phase is dubbed the representation SPT (RSPT) state.
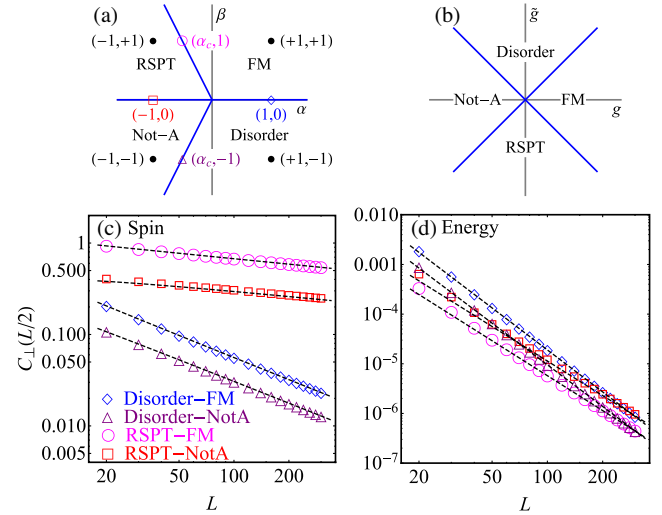

FIG. 3. (a) Schematic quantum phase diagram of the generalized Potts chain. The special points $(\alpha, \beta) = (\pm 1, \pm 1)$ are marked by filled circles. The QCPs studied in this Letter are indicated on the transition lines, in which $\alpha_c = -0.505\,09$. (b) Global phase diagram of the effective field theory (12). (c) and (d) Connected correlation functions $C_\perp(L/2)$ of the spin operator σ_l and the energy operator $\epsilon_l = \tau_l + \tau_l^\dagger$ at the QCPs. Dashed lines are the power-law fitting according to Eq. (2) plus a correction-to-scaling term, $bL^{-\Delta_\phi - \Delta_\phi^b - 1}$.

At $(\alpha, \beta) = (-1, 1)$, its ground state can be constructed with the matrix-product state $R = \otimes_l R_l$, in which

$$R_l = \begin{pmatrix} |0\rangle_l & |+\rangle_l \\ |-\rangle_l & |0\rangle_l \end{pmatrix}. \quad (11)$$

Here, $|0\rangle$, $|+\rangle$, and $|-\rangle$ are the three eigenstates of S^z. The ground state is given by $\mathrm{tr}(R)$ for periodic B.C., which is S_3-symmetric and nondegenerate. With open B.C., the matrix elements of R are fourfold degenerate ground states, which form a linear representation of the S_3 symmetry.

The duality transformation $\tau_l \mapsto \sigma_l^\dagger \sigma_{l+1}$, $\sigma_l \mapsto \prod_{j=1}^l \tau_j$ exchanges the two terms in H_P and leaves H_0 invariant, thus maps the FM to the disordered phase, and the not-A order to the RSPT phase, and vice versa. There is a continuous quantum phase transition between each ordered phase and each disordered phase, all of which correspond to the spontaneous S_3-symmetry breaking and belong to the 2D three-state Potts universality class. These transition lines join at the multicritical point $(\alpha, \beta) = (0, 0)$, which is self-dual and has the U(1) symmetry generated by $Q = \sum_l S_l^z$.

The phase diagram is captured by the following self-dual sine-Gordon theory with the Hamiltonian density [see Fig. 3(b)],

$$\mathcal{H} = \frac{3}{4\pi}(\partial_x \phi)^2 + \frac{3}{4\pi}(\partial_x \theta)^2 - g\cos(3\phi) - \tilde{g}\cos(3\theta), \quad (12)$$

in which ϕ and θ are the scalar field and the dual disorder field, respectively. The multicritical point is captured by the free boson theory with a compactification radius $\sqrt{3/2}$, which has the same U(1) symmetry and self-duality [41,55]. The g and $\tilde{g}$ terms are relevant at the multicritical point. For $g > |\tilde{g}| > 0$, ϕ is polarized to 0 or $\pm 2\pi/3$ and gives the FM order, while for $g < -|\tilde{g}| < 0$, ϕ is polarized to π or $\pm\pi/3$, i.e., an equal-weight superposition of two out of the three spin states, and describes the not-A order.

For $\tilde{g} > |g| > 0$, the disorder field θ is pinned at 0 or $\pm 2\pi/3$, while for $\tilde{g} < -|g| < 0$, θ is pinned at π or $\pm\pi/3$. From the duality relation, the former corresponds to the disordered phase, while the latter is the RSPT phase. The transition lines are given by $|g| = |\tilde{g}|$, which cannot be smoothly connected without either crossing the multicritical point or explicitly breaking the S_3 symmetry despite that they belong to the same universality class. However, unlike the CI chain, there are not any degenerate edge states at these QCPs, thus we must find new characteristics.

Generalized Potts chain: Conformal B.C.—We first study the surface critical behavior. The connected correlation functions of the spin operator σ_l and the energy operator $\epsilon_l = \tau_l + \tau_l^\dagger$ are calculated with the density-matrix renormalization group algorithm [56–58] detailed in [42] and shown in Fig. 3. The scaling dimensions of the boundary operators are extracted by fitting Eq. (2) with $\Delta_\sigma^b = 2/15$ and $\Delta_\epsilon^b = 2$ and listed in Table I. The four QCPs fall into two classes. While the disorder-FM and the disorder-NotA transitions are captured by the Potts CFT with free B.C. [21], the RSPT-FM and the RSPT-NotA transitions yield different critical exponents. It turns out that these exponents can be derived from the Potts CFT with the "new" conformal B.C. discovered in Refs. [59,60]. This B.C. is S_3 symmetric and dual to the mixed B.C. [61], thus we call it the dual-mixed B.C.

In order to support the identification of these conformal B.C., we show the low-energy spectra at these QCPs with open B.C. in Fig. 4, which are normalized to the effective scaling dimensions. The spectra of the disorder-FM and the disorder-NotA QCPs are consistent with the operator content of the Potts CFT with free B.C. On the other hand, the spectra of the RSPT-FM and the RSPT-NotA QCPs are consistent with the dual-mixed B.C.

The operator content of a boundary CFT also shows up in the entanglement spectrum of the ground state, which is equivalent to the energy spectrum of the CFT with a proper conformal B.C. specified at the entangling surface, i.e., the
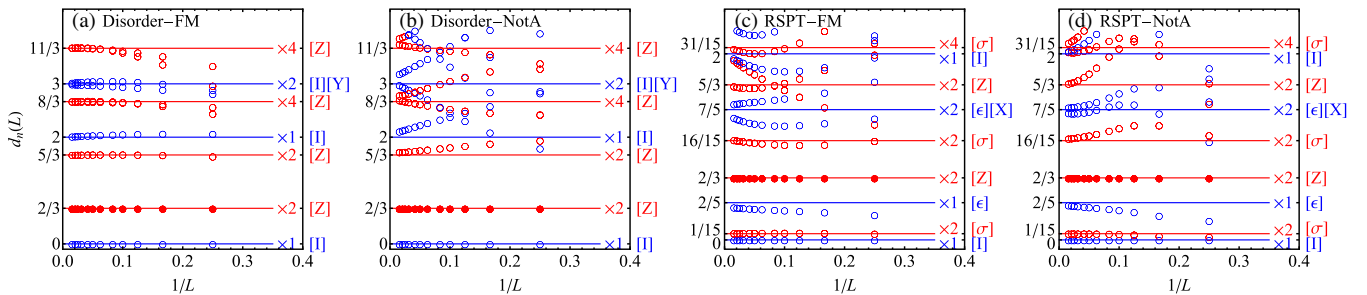

FIG. 4. Low-energy spectra of the generalized Potts chain at the QCPs. The excitation energy $\Delta\epsilon_n(L) = \epsilon_n(L) - \epsilon_0(L)$ is normalized to the effective scaling dimension, $d_n(L) = \frac{2}{3}[\Delta\epsilon_n(L)/\Delta\epsilon_Z(L)]$, such that the primary state in $[Z]$ (marked with filled circles) is normalized to $2/3$. The conformal family and the expected degeneracy in the boundary CFT are labeled on the right. Red circles indicate numerically exactly twofold degenerate levels, while blue circles indicate nondegenerate levels. The disorder-FM and the disorder-NotA QCPs are consistent with the operator content of the Potts CFT with free B.C. [21], $\mathbb{I} \oplus [Y] \oplus 2[Z]$, while the RSPT-FM and the RSPT-NotA QCPs are consistent with that of the dual-mixed B.C. [59,60], $\mathbb{I} \oplus [Y] \oplus [\epsilon] \oplus [X] \oplus 2[\sigma] \oplus 2[Z]$.

boundary between the subsystem and the rest of the chain [62–64]. The entanglement spectra of the generalized Potts chain are shown in Supplemental Material [42], which points to the same operator contents as the corresponding energy spectra.

These distinct conformal B.C. can be derived from the bulk effective field theory (12). Given that the disorder-FM transition at $g = \tilde{g} > 0$ realizes the free B.C. [21], the dual field θ is pinned at 0 or $\pm 2\pi/3$ at the boundary due to the duality between the free B.C. and the fixed B.C. [65]. At the RSPT-FM transition for $\tilde{g} = -g < 0$, the sign of $\tilde{g}$ is reversed, thus θ is pinned at π or $\pm\pi/3$ at the boundary, corresponding to the mixed B.C. of the θ field and thus the dual-mixed B.C. in terms of the ϕ field. On the other hand, the conformal B.C. is not changed by reversing the sign of g, because the ϕ field is not polarized at the boundary for any of these critical states. Therefore, the disorder-NotA transition at $g = -\tilde{g} < 0$ realizes the free B.C., while the RSPT-NotA transition at $g = \tilde{g} < 0$ shows the dual-mixed B.C. These arguments are consistent with our numerical results, thereby we establish a novel bulk-boundary correspondence of the symmetry-enriched quantum critical states.

Discussions.—The critical exponents of the boundary correlation functions can be measured with the surface magnetic susceptibility, etc. [24]. Besides, the characteristic energy spectrum manifests itself in thermodynamic quantities. The thermal entropy of a critical chain of length L at temperature T scales as [66]

$$S(L,T) = \frac{\pi c}{3v} LT + \ln g, \qquad (13)$$

in which c is the central charge, v is the velocity in the low-energy limit, and $\ln g$ is the Affleck-Ludwig boundary entropy, which is a universal constant determined by the conformal B.C. The excess boundary entropy of a conformal B.C. compared with the fixed B.C. can be extracted from the entropy released upon applying a magnetic field on the boundary. If there are degenerate edge states, they contribute an integer factor of degeneracy to g, while g is not an integer for a generic conformal B.C. but may be taken as an "effective edge degeneracy." Therefore, the conformal B.C. generalizes the edge degeneracy in characterizing quantum critical states.

Conclusion.—To summarize, we have studied the generalized Ising and Potts chains. In each family, we focused on the quantum critical states that cannot be smoothly connected even though they are captured by the same CFT. We showed that a distinct conformal B.C. is realized at the QCPs of SPT states. The conformal B.C. is a more generic characteristic of symmetry-enriched quantum critical states beyond the degenerate edge states.

We thank Paul Fendley, Shang Liu, Rong-Yang Sun, Huajia Wang, and Yijian Zou for helpful discussions and

---

*These authors contributed equally to this work.
†longzhang@ucas.ac.cn

[1] X.-G. Wen, Rev. Mod. Phys. **89**, 041004 (2017).
[2] Z.-C. Gu and X.-G. Wen, Phys. Rev. B **80**, 155131 (2009).
[3] F. Pollmann, A. M. Turner, E. Berg, and M. Oshikawa, Phys. Rev. B **81**, 064439 (2010).
[4] A. Keselman and E. Berg, Phys. Rev. B **91**, 235309 (2015).
[5] T. Scaffidi, D. E. Parker, and R. Vasseur, Phys. Rev. X **7**, 041048 (2017).
[6] R. Verresen, R. Thorngren, N. G. Jones, and F. Pollmann, Phys. Rev. X **11**, 041059 (2021).
[7] M. Cheng and H.-H. Tu, Phys. Rev. B **84**, 094503 (2011).
[8] L. Fidkowski, R. M. Lutchyn, C. Nayak, and M. P. A. Fisher, Phys. Rev. B **84**, 195436 (2011).
[9] J. D. Sau, B. I. Halperin, K. Flensberg, and S. Das Sarma, Phys. Rev. B **84**, 144509 (2011).
[10] J. P. Kestner, B. Wang, J. D. Sau, and S. Das Sarma, Phys. Rev. B **83**, 174409 (2011).
[11] F. Iemini, L. Mazza, D. Rossini, R. Fazio, and S. Diehl, Phys. Rev. Lett. **115**, 156402 (2015).
[12] N. Lang and H. P. Büchler, Phys. Rev. B **92**, 041118(R) (2015).
[13] J. Ruhman and E. Altman, Phys. Rev. B **96**, 085133 (2017).
[14] H.-C. Jiang, Z.-X. Li, A. Seidel, and D.-H. Lee, Sci. Bull. **63**, 753 (2018).
[15] D. E. Parker, T. Scaffidi, and R. Vasseur, Phys. Rev. B **97**, 165114 (2018).
[16] A. Keselman, E. Berg, and P. Azaria, Phys. Rev. B **98**, 214501 (2018).
[17] R. Verresen, N. G. Jones, and F. Pollmann, Phys. Rev. Lett. **120**, 057001 (2018).
[18] N. G. Jones and R. Verresen, J. Stat. Phys. **175**, 1164 (2019).
[19] R. Verresen, arXiv:2003.05453.
[20] R. Thorngren, A. Vishwanath, and R. Verresen, Phys. Rev. B **104**, 075132 (2021).
[21] J. L. Cardy, Nucl. Phys. **B275**, 200 (1986).
[22] J. L. Cardy, Nucl. Phys. **B324**, 581 (1989).
[23] J. L. Cardy, Nucl. Phys. **B240**, 514 (1984).
[24] K. Binder, in *Phase Transitions and Critical Phenomena*, edited by C. Domb and J. L. Lebowitz (Academic Press, London, England, 1983), Vol. 8.

[25] H. W. Diehl, in *Phase Transitions and Critical Phenomena*, edited by C. Domb and J. L. Lebowitz (Academic Press, London, 1986), Vol. 10.

[26] T. Grover and A. Vishwanath, arXiv:1206.1332.

[27] T. Suzuki and M. Sato, Phys. Rev. B **86**, 224411 (2012).

[28] L. Zhang and F. Wang, Phys. Rev. Lett. **118**, 087201 (2017).

[29] C. Ding, L. Zhang, and W. Guo, Phys. Rev. Lett. **120**, 235701 (2018).

[30] L. Weber, F. Parisen Toldin, and S. Wessel, Phys. Rev. B **98**, 140403(R) (2018).

[31] L. Weber and S. Wessel, Phys. Rev. B **100**, 054437 (2019).

[32] L. Weber and S. Wessel, Phys. Rev. B **103**, L020406 (2021).

[33] W. Zhu, C. Ding, L. Zhang, and W. Guo, Phys. Rev. B **103**, 024412 (2021).

[34] C. Ding, W. Zhu, W. Guo, and L. Zhang, arXiv:2110.04762.

[35] F. Parisen Toldin, Phys. Rev. Lett. **126**, 135701 (2021).

[36] M. Hu, Y. Deng, and J.-P. Lv, Phys. Rev. Lett. **127**, 120603 (2021).

[37] F. Parisen Toldin and M. A. Metlitski, Phys. Rev. Lett. **128**, 215701 (2022).

[38] C.-M. Jian, Y. Xu, X.-C. Wu, and C. Xu, SciPost Phys. **10**, 033 (2021).

[39] M. Metlitski, SciPost Phys. **12**, 131 (2022).

[40] J. Padayasi, A. Krishnan, M. Metlitski, I. Gruzberg, and M. Meineri, SciPost Phys. **12**, 190 (2022).

[41] E. O'Brien, E. Vernier, and P. Fendley, Phys. Rev. B **101**, 235108 (2020).

[42] See Supplemental Material at http://link.aps.org/supplemental/10.1103/PhysRevLett.129.210601, which also include Refs. [43–54] for details of numerical calculations.

[43] M. Fishman, S. R. White, and E. M. Stoudenmire, arXiv:2007.14822.

[44] F. Verstraete, V. Murg, and J. Cirac, Adv. Phys. **57**, 143 (2008).

[45] F. Verstraete and J. I. Cirac, Phys. Rev. B **73**, 094423 (2006).

[46] J. Haegeman and F. Verstraete, Annu. Rev. Condens. Matter Phys. **8**, 355 (2017).

[47] V. Zauner-Stauber, L. Vanderstraeten, M. T. Fishman, F. Verstraete, and J. Haegeman, Phys. Rev. B **97**, 045145 (2018).

[48] M. Rader and A. M. Läuchli, Phys. Rev. X **8**, 031030 (2018).

[49] P. Corboz, P. Czarnik, G. Kapteijns, and L. Tagliacozzo, Phys. Rev. X **8**, 031031 (2018).

[50] P. Calabrese and J. Cardy, J. Stat. Mech. (2004) P06002.

[51] P. Calabrese and J. Cardy, J. Phys. A **42**, 504005 (2009).

[52] V. Alba, P. Calabrese, and E. Tonni, J. Phys. A **51**, 024001 (2018).

[53] A. Kitaev and J. Preskill, Phys. Rev. Lett. **96**, 110404 (2006).

[54] M. Levin and X.-G. Wen, Phys. Rev. Lett. **96**, 110405 (2006).

[55] D. Baranowski and V. Rittenberg, J. Phys. A **23**, 1029 (1990).

[56] S. R. White, Phys. Rev. Lett. **69**, 2863 (1992).

[57] U. Schollwöck, Rev. Mod. Phys. **77**, 259 (2005).

[58] U. Schollwöck, Ann. Phys. (N. Y). **326**, 96 (2011).

[59] I. Affleck, M. Oshikawa, and H. Saleur, J. Phys. A **31**, 5827 (1998).

[60] J. Fuchs and C. Schweigert, Phys. Lett. B **441**, 141 (1998).

[61] With the mixed B. C., the edge spin is polarized as an equal-weight superposition of two out of the three spin states with the edge order $\langle\sigma\rangle^3 < 0$.

[62] A. M. Läuchli, arXiv:1303.0741.

[63] K. Ohmori and Y. Tachikawa, J. Stat. Mech. (2015) P04010.

[64] J. Cardy and E. Tonni, J. Stat. Mech. (2016) 123103.

[65] K. Drühl and H. Wagner, Ann. Phys. (N.Y.) **141**, 225 (1982).

[66] I. Affleck and A. W. W. Ludwig, Phys. Rev. Lett. **67**, 161 (1991).